# Method of Assessing Voltage Response of Inverter-Based Generation Due to System Faults

Douglas Bowman, P.E.
Southwest Power Pool
Little Rock AR, USA
dbowman@spp.org

Roy A. McCann
University of Arkansas
Fayetteville AR, USA
rmccann@uark.edu

Nathan Bean
Southwest Power Pool
Little Rock AR, USA
nbean@spp.org

***Abstract*— The increasing capacity from inverter-based resources (IBR) creates challenges for designing and operating electric power systems. In particular, wind and solar generation has very different characteristics compared to conventional turbo generators. This research investigates the critical clearing times for IBR as larger amounts of wind generation brought online. This paper develops a new six-bus transmission test systems for which multiple wind stations are interconnected. An exhaustive study of fault locations with respect to load levels and line impedances for a wide range of IBR penetration levels was performed with respect to inverter stability analysis to determine the corresponding critical clearing times. The results show that voltage stability at IBR points of interconnection can occur at not only higher penetration levels, but at lower penetrations as well.**

***Keywords—critical clearing time, faults, inverter-based resources, short circuit ratio, wind penetration, voltage stability***

## I. Introduction

As the power industry continues on its journey toward near 100% renewables, inverter based power electronics devices are being more widely deployed. Wind, solar, as well as battery storage make up the majority of these resources. Southwest Power Pool (SPP), a Regional Transmission Organization (RTO), now has over 24 GW of wind capacity, and another 53GW of wind and 37GW of solar being studied through the Generator Interconnection (GI) Process to serve an off-peak load of nearly 21GW. SPP's current renewables penetration record is 78.2% and a wind penetration record of 73.2% was realized in April, 2020. Moreover, there are occasions during these events where up to 2GW was curtailed.

High wind penetration studies have been published providing much needed results and recommendations for the research community as well as industry [1]. Indeed, SPP has completed multiple studies to analyze the stability impact of high wind penetrations. The most recent SPP study is termed the Inverter Based Generator Integration Study (IBIS). The goal of the IBIS study was to determine the existence (if any), the cause, and the impact of inverter controls interactions due to grid weakness and high levels of IBR on system stability within the SPP footprint [2]-[3]. These papers reveal the impact of short circuit ratios (SCR, WSCR, and CSCR) and critical clearing times of IBR due to point of interconnection (POI) faults. The final result noted inverter instability is indeed possible. Today, assurance of inverter stability cannot be preserved due to insufficient generic and user-written positive sequence dynamics models. Work is currently being accomplished by NERC, WECC, and EPRI to deliver models that are more accurate in terms of dynamic response.

When IBR is connected to the transmission system, acceptable voltages must be maintained at the point of interconnection (POI). Nearby faults can cause voltage instability of the wind plant. A number of papers have been written addressing the issue [4]-[6], providing methods to increase the voltage stability using wind turbine voltage control strategies. This paper provides detailed data and study results for a six bus system used to produce multiple power flow/dynamics models by varying multiple parameters. Short circuit ratios and critical clearing times are calculated and dynamics simulations are implemented to determine the relationships among the parameters and how voltage stability is impacted. Part II gives the details of the modeling effort for the system under study. Part III discussed the calculation of both the short circuit ratios and the critical clearing times for IBRs for all models and Part IV provides a dialogue on the dynamics simulation of fault events. The results of the calculations and simulations are given in Part V. The results are summarized and conclusions are drawn in Part VI.

## II. Models

### A. Base Model Construction

The 138 kV six bus system shown in Fig. 1 was developed using Siemens PTI's PSS®E version 33.10 software and SPP system data. PSS®E is used worldwide by power system planners for grid simulations and analysis and is one of the most popular in the industry. The base system is set at 30% wind penetration and consists of six 138 kV buses connected via seven 138 kV transmission lines of various lengths, one conventional gas plant, one conventional coal plant, two DFIG wind plants, and four loads. Note the 138 kV system in red.

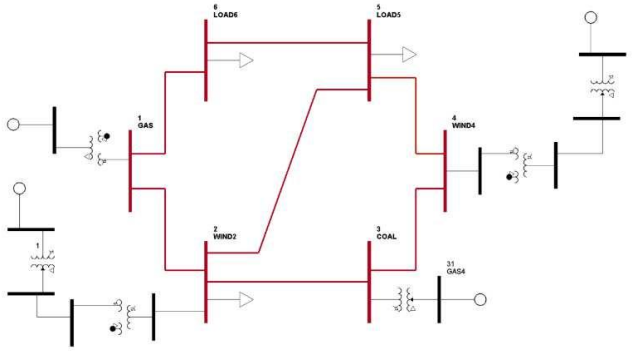


Fig. 1. Six bus system one-line diagram.

2166-5478/21/$31.00 ©2021 IEEE
DOI 10.1109/GreenTech48523.2021.00082

The transmission lines are taken from actual power flow data in SPP models to obtain a good representation of the various line lengths and impedances of a real system. The system loads are taken from SPP models as well to get a fair representation of actual bus MVA loads. The two conventional generators shown are generators in the SPP system, one a gas-fired plant and the other a coal plant. The two wind plants are representations of actual wind interconnections to the SPP system. As per Fig. 1, and in order to get a true depiction, generator step up transformers, collector systems, three-winding substation transformers, and interconnection lines were included for the wind plant for completeness. The power flow data is shown in Tables I and II.

TABLE I. BASE SYSTEM GENERATOR AND LOAD DATA

| Bus No. | Base kV | Pgen MW | Pmax MW | Qgen MVar | Qmax MVar | Pload MW | Qload MVar |
|---|---|---|---|---|---|---|---|
| 2 | 138.0 | ---- | ---- | ---- | ---- | 38.0 | 22.0 |
| 5 | 138.0 | ---- | ---- | ---- | ---- | 90.0 | 34.0 |
| 6 | 138.0 | ---- | ---- | ---- | ---- | 66.0 | 17.0 |
| 12 | 13.8 | 65.0 | 83.44 | 17.20 | 17.20 | ---- | ---- |
| 25 | 0.7 | 30.0 | 80.0 | 36.46 | 36.46 | ---- | ---- |
| 31* | 13.8 | 75.18 | 88.0 | 26.09 | 56.0 | ---- | ---- |
| 45 | 0.7 | 28.20 | 100.0 | 9.27 | 9.27 | ---- | ---- |

*swing bus

The buses shown above in Table I are those where generators or loads are connected. All other buses are omitted, however, they are shown in Fig. 1.

TABLE II. BASE SYSTEM BRANCH DATA

| From Bus | To Bus | To Bus | R (pu) | X (pu) | B (pu) | Line Length (miles) |
|---|---|---|---|---|---|---|
| 1 | 2 | ---- | 0.010690 | 0.047000 | 0.013760 | 12.25 |
| 1 | 6 | ---- | 0.034230 | 0.074900 | 0.017090 | 17.28 |
| 2 | 3 | ---- | 0.008361 | 0.059166 | 0.016520 | 15.0 |
| 2 | 5 | ---- | 0.024660 | 0.140000 | 0.040260 | 36.0 |
| 3 | 4 | ---- | 0.020750 | 0.120290 | 0.032550 | 30.20 |
| 4 | 5 | ---- | 0.013800 | 0.080000 | 0.022180 | 20.28 |
| 5 | 6 | ---- | 0.023940 | 0.072480 | 0.018080 | 17.5 |
| 2 | 21 | ---- | 0.003225 | 0.023583 | 0.006790 | 6.13 |
| 4 | 41 | ---- | 0.000007 | 0.000040 | 0.000010 | 0.01 |
| 22 | 24 | ---- | 0.010850 | 0.013410 | 0.032900 | 19.6 |
| 42 | 44 | ---- | 0.007790 | 0.011190 | 0.009070 | 1.0 |
| 24 | 25 | ---- | 0.005820 | 0.065740 | ---- | 2WTxf |
| 3 | 31 | ---- | 0.005300 | 0.106000 | ---- | 2WTxf |
| 44 | 45 | ---- | 0.007500 | 0.060000 | ---- | 2WTxf |
| 21 | 22 | 23 | 0.00161<br>0.00058 | 0.08699<br>0.03129 | 0.0008 | 3WTxf |
| | | | 0.0023 | 0.12448 | | |
| 42 | 41 | 43 | 198636.8<br>456336.6<br>370410.8 | 0.0881<br>0.147<br>0.0378 | 0.00075 | 3WTxf |
| 12 | 1 | 13 | 109995<br>71241<br>98311.01 | 0.1174<br>0.1107<br>0.2014 | 0.00189 | 3WTxf |

Note: 3WTxf data in p.u. or Watts

Generator dynamics data was also applied in this study and is shown in Table III. Multiple dynamics models are used for each wind generator and the actual dynamics models are provided for the associated gas, coal, or wind plant. In this study, the wind plant models are 2nd generation WECC generic type 3.

### *B. Construction of Additional Models*

A number of additional models were produced using the base model as a foundation by varying wind penetration, load, and line lengths. The total number of models constructed was $5^3$=125, which was all possible combinations of penetration, loads, and line lengths. Table III shows the parameter ranges.

TABLE III. PARAMETER RANGES

| PARAMETER | VALUE | | | | |
|---|---|---|---|---|---|
| Wind Penetration (%) | 30% | 45% | 60% | 75% | 90% |
| System Load (MVA) | 97+j36.5 | 121.25+j45.63 | 145.5+j54.75 | 169.75+j63.88 | 194+j73 |
| Total Lines Length (miles) | 148.51 | 185.64 | 222.76 | 259.89 | 297.02 |

When each set of load changes were made to a particular model, the corresponding wind MW output was necessarily changed to provide the correct wind penetration level according to (1).

$$Wind\ Penetration = \frac{Wind\ Power\ MW}{Load\ MW} x100\% \qquad (1)$$

## III. SCR AND CCT CALCULATIONS

The 125 models were first evaluated using EPRI's Grid Strength Assessment Tool (GSAT) [7]. GSAT was developed by the Electric Power Research Institute (EPRI) as a screening tool to provide the engineer with an indication of short circuit strength at buses of interest. IBR critical clearing times (CCT) can also be calculated by the tool to assess inverter stability as shown in [3] and [8]. Benchmarking of the tool against point-on-wave time domain simulations was performed in [3]. Benchmark results demonstrated that the CCTs calculated by GSAT were reasonably accurate.

### A. Short Circuit Ratio

Short Circuit Ratio (SCR) is the conventional method for calculating short circuit strength, however, when two or more IBRs are connected electrically close, the Weighted Short Circuit Ratio (WSCR) and Composite Short Circuit Ratio (CSCR) give a better indication of the strength [9]-[10]. The GSAT tool can calculate all three ratios.

The ratios were calculated using GSAT for wind POI buses 2 and 4 for all 125 models. Ratios at other buses were not calculated as our interest pertains exclusively to IBR locations.

### B. Critical Clearing Time

The CCT in the context of IBR stability can be defined as the maximum time a fault near the POI of the inverter plant is allowed to remain on the system to eliminate the possibility of instability of the inverter plant. This instability is normally due to loss of inverter synchronism causing large oscillations and increased settling times in voltage and powers. These oscillations can cause tripping of the wind plant [8].

The CCTs were calculated using GSAT for all 125 models for wind plant POI buses 2 and 4. CCTs at other buses were not calculated as our interest applies exclusively to IBR locations.

It was presented in [8] that WTG stability is directly related to the phase-locked loop and terminal voltage controller gain values. For this study, the control parameters for the two wind plants are given in Table IV.

TABLE IV. CONTROL PARAMETERS

| Wind Turbine Generator Bus | PLL | | | | Voltage Controller | |
|---|---|---|---|---|---|---|
| | $K_i$ | $K_p$ | $f_{max}$ | $f_{min}$ | $K_{vi}$ | $K_{vp}$ |
| 25 | 1400 | 60 | 72 Hz | 48 Hz | 120 | 1 |
| 45 | 1400 | 60 | 72 Hz | 48 Hz | 40 | 0 |

## IV. DYNAMICS SIMULATIONS

Dynamics Simulations were performed in PSS®E to assess the transient stability of the inverter plants due to system fault events. Three phase faults were applied to all 138kV buses for all models with clearing times ranging from 8 cycles to 16 cycles by using the steps shown in the following example:

1. Run the simulation for 0.5 seconds
2. Apply a three phase fault at the 138kV bus
3. Run the simulation for 10 cycles (0.167 sec)
4. Remove the three phase fault
5. Trip one 138kV branch
6. Run the simulation to 10 seconds

Since each bus had more than one connected line, the fault was applied to the bus in separate simulations, the number of which was according to the number of connected lines. In all, the number of dynamics simulations was 8750, which accounted for 125 models consisting of combinations of all wind penetrations, system load, and line length according to Table IV as well as five different clearing times for each of fourteen bus faults. Therefore, the 8750 simulations is readily understood as seventy faults applied to each of the 125 models.

## V. RESULTS

### A. Short Circuit Ratio Calculation Results

The SCRs calculated for POI buses 2 and 4 are shown in Figs. 2 and 3. WSCRs and CSCRs were not calculated as the two plants were deemed electrically distant.

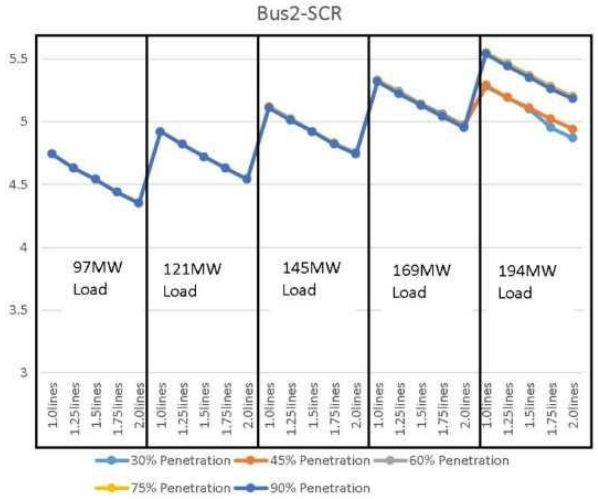


Fig. 2. Short circuit ratios for bus 2

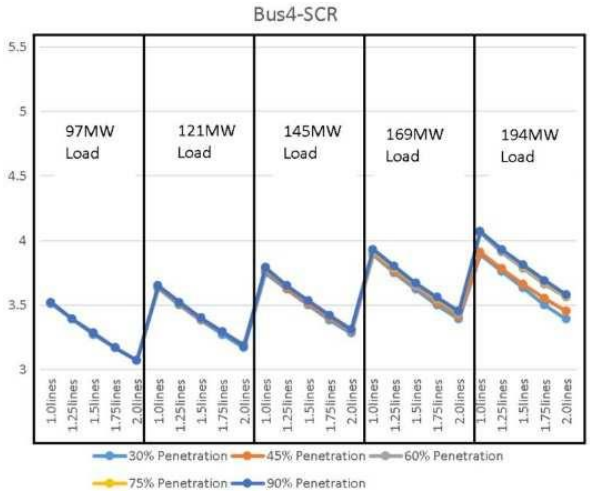


Fig. 3. Short circuit ratios for bus 4.

A few observations can be made according the figures.

- SCRs experienced little change at wind penetrations below 90%. The SCRs are, however, lower by approximately 30% when the load is doubled and penetration is below 60%
- SCRs at bus 4 are approximately 25% to 30% lower than those of bus 2, meaning bus 4 is weaker by said percentages. This is reasonable since the MW rating of wind plant WG2 is 25% lower than that of the wind plant WG4.
- SCRs at both buses are considered low since the threshold for weakness in this analysis is 6.0.

### B. *Critical Clearing Time Calculation Results*

The CCTs were calculated for wind plant POIs at buses 2 and 4. Results are shown in Fig. 4 and 5.

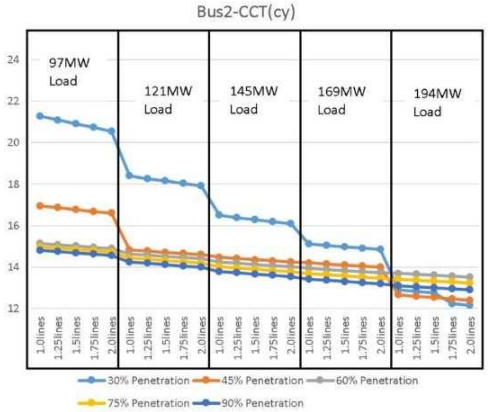


Fig. 4. Critical clearing times for bus 2.

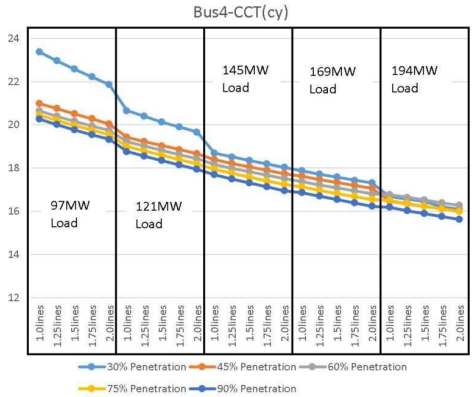


Fig. 5. Critical clearing times for bus 4.

Observations for these calculations show:

- CCTs are reduced as wind penetrations increase, except at maximum load
- CCTs are reduced as load increases
- CCTs are reduced as line lengths increase
- CCTs flatten for wind penetrations above 45%
- CCTs for 30% and 45% penetrations drop below the higher penetrations at maximum load level
- CCTs at bus 4 are approximately 20% higher than those of bus 2.

### C. *Dynamics Simulations Results*

The longest clearing time used in the dynamics simulations was 16 cycles. According to Fig. 4, 105 of the 125 models had CCTs for WTG 25 that were between 12 and 16 cycles for bus 2. Therefore, as a conservative measure, only the simulations with clearing times of 16 cycles were examined for these 105 models.

Since our purpose is to examine inverter stability for the wind plants, focus was given to voltages at POI bus 2 and its connected transmission lines. Analyses was done to determine which line connected to bus 2 would, subsequent to tripping, offer the more severe voltage response. It was found through random testing on multiple models that tripping line 2-3 would be more severe than line 1-2 or line 2-5, the results of which are shown in Fig. 6. Therefore, all simulations with tripping of the latter two lines were omitted from further investigation.

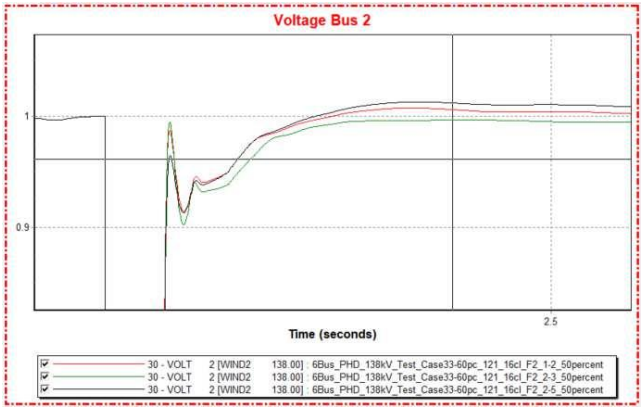


Fig. 6. Response of tripped lines for a fault at bus 2.

To understand the impact of increasing wind penetration on voltage at bus 2, comparisons were made at all penetrations for low and high load levels. The line lengths are at maximum length and 16 cycle faults were applied. Fig. 7 and Fig. 8 show the results for low load and high load respectively.

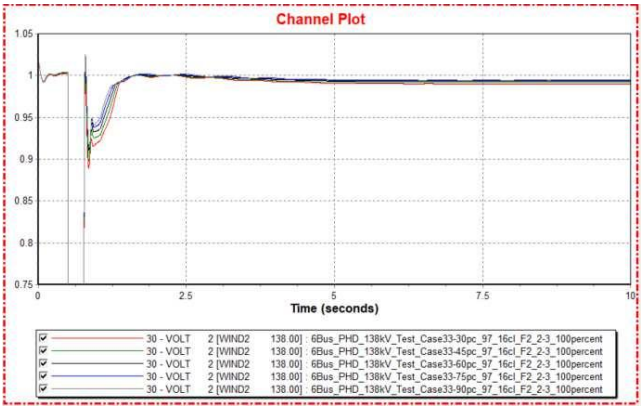


Fig. 7. Bus 2 voltage responses for varying wind penetration at low load

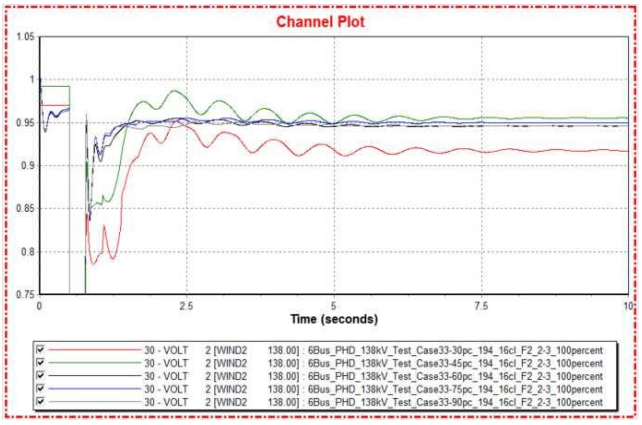


Fig. 8. Bus 2 voltage responses for varying wind penetration at high load.

The voltage responses at bus 2 are shown in Fig. 9 as load is varied for 30% wind penetration and Fig. 10 for 90% wind penetration. Sixteen cycle faults were applied and maximum line lengths were used.

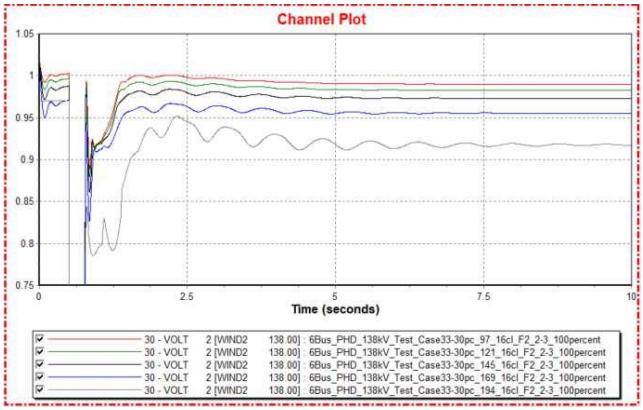


Fig. 9. Bus 2 voltage responses with varying load and low wind penetration.

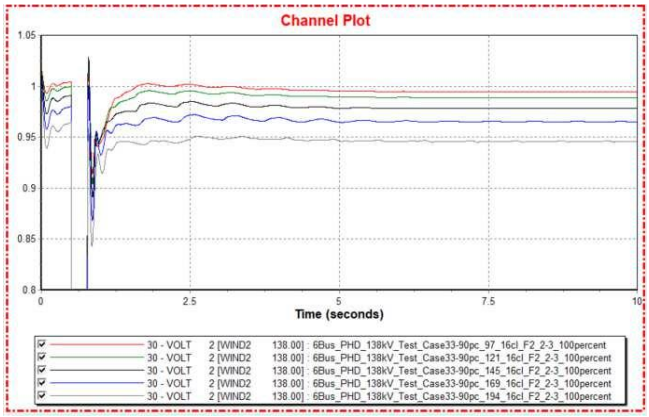


Fig. 10. Bus 2 voltage responses with varying load and high wind penetration.

Examining the Figs. 7 through 10 reveals the following:

- At low load, voltage responses vary little as wind penetration increases; however, as Fig. 7 shows, the lower penetrations have a slightly more severe response.
- According to Fig. 8, at the high load, voltage responses as wind penetration vary are more severe at the lower penetrations.
- At a low wind penetration of 30%, the voltage responses shown in Fig. 9 are more severe for higher loads.
- Fig 10 shows that at a high wind penetration of 90%, the voltage responses at higher loads are, similar to 30%, more severe. However, the overall voltage response is better.

The SCRs and CCTs at bus 2 and bus 4 have an inverse relationship, that is, bus 2 has the higher SCRs and the lower CCTs while bus 4 has the lower SCRs and the higher CCTs. This agrees with the conclusion drawn in [3] that the two parameters are weakly correlated. However, this does not mean that other systems would demonstrate the same inverse relationship.

The fault at bus 2 with outage of line 2-3 is the most critical. At low penetrations, the event causes very low voltages at bus 2 when the load is maximum. Furthermore, assessing the outage of the line in steady state power flow reflects voltage collapse. This is due to the load at bus 2 being radially connected at the end of the 138kV system after the event occurs. Reactive power resources aren't available to assist in recovery.

Additionally, one can see the relationship between the calculated SCRs/CCTs and the voltage response in the preceding discussion. At high load, with penetrations at 30% and 45%, the CCTs for bus 2 in Fig. 4-- fall below those of the higher penetrations. When comparing these CCTs with the voltage responses of Fig. 7 and Fig. 8 as discussed, it is easy to see the correlation. It is reasonable to infer that lower CCTs can predict voltage instability.

This is all of course an artifact of the models with their many parameters. For instance, had the fault event occurred with stronger system sources and lower system impedances, the voltage issue may not have occurred.

## VI. Summary And Concusion

SCR and CCT calculations were performed on multiple models having a combination of different parameters. Dynamic simulations were then performed to ascertain the impact of a multitude of fault events on voltage stability. It was found that voltage issues and even voltage collapse can occur at low as well as high wind penetration levels, especially with high loads.

## References


[1] J. DeCesaro, K. Porter, M. Milligan, "Wind Energy and Power Systems Operations: A Review of Wind Integration Studies to Date"' *The Electricity Journal*, Volume 22, Issue 10, 2009, pp. 34-43

[2] D. Bowman, D. Ramasubramanian, R. McCann, E. Farantatos, A. Gaikwad, J. Caspary, "SPP Grid Strength Study with High Inverter-Based Resource Penetration," *2019 North American Power Symposium* (NAPS), Wichita, KS, 2019.

[3] W. Wang, D. Ramasubramanian, E. Farantatos, D. Bowman, H. Scribner, J. Tanner, C. Cates, J. Caspary, A. Gaikwad, "Evaluation of Inverter Based Resources Transient Stability Performance in Weak Areas in Southwest Power Pool's System Footprint" *CIGRE Session 48*, Paris, 2020.

[4] E. Vittal, M. O'Malley and A. Keane, "A Steady-State Voltage Stability Analysis of Power Systems With High Penetrations of Wind," *IEEE Transactions on Power Systems,* vol. 25, no. 1, pp. 433-442, Feb. 2010.

[5] Y. Li, L. Fan and Z. Miao, "Stability Control for Wind in Weak Grids," *IEEE Transactions on Sustainable Energy*, vol. 10, no. 4, pp. 2094-2103, Oct. 2019.

[6] S. Ma, H. Geng, L. Liu, G. Yang and B. C. Pal, "Grid-Synchronization Stability Improvement of Large Scale Wind Farm During Severe Grid Fault," *IEEE Transactions on Power Systems*, vol. 33, no. 1, pp. 216-226, Jan. 2018.

[7] Electric Power Research Institute: "PRE-SW: Grid Strength Assessment Tool (GSAT) v2.1", Palo Alto, CA, 2019, 3002017456

[8] Electric Power Research Institiute, "Guidelines for Studies on Weak Grids with Inverter Based Resources," Palo Alto, CA, December 2018.

[9] NERC, "Integrating Inverter Based Resources into Weak Power Systems, Reliability Guideline", June 2017

[10] Y., Zhang, et. al, "Evaluating system strength for large-scale wind plant integration", *2014 IEEE PES General Meeting*, National Harbor, MD, 2014